International Journal of Remote Sensing
Vol. 29, Nos. 17–18, September 2008, 5397–5408

Taylor & Francis
Taylor & Francis Group

Effective versus measured correlation length for radar-based surface soil moisture retrieval

J. ÁLVAREZ-MOZOS*, M. GONZÁLEZ-AUDÍCANA, J. CASALÍ and A. LARRAÑAGA

Public University of Navarre, Department of Projects and Rural Engineering, Arrosadia s/n, 31006 Pamplona, Spain

(*Received 1 December 2006; in final form 3 July 2007*)

At present, radar-based surface soil moisture (*SM*) retrieval is hampered by the influence of surface roughness on the backscattering coefficient (σ^0). Surface roughness is typically represented by two parameters, namely the standard deviation of surface heights (*s*) and the surface correlation length (*l*). The latter is a very problematic parameter, since it is extremely variable and very difficult to measure adequately. Therefore, several authors proposed calibrating it using backscattering models yielding *optimum* or *effective l* values. Baghdadi *et al.* found that those *effective l* were related to the parameter *s* and the configuration of the sensor, and proposed an approach to calculate it. The objective of this study is to evaluate the validity of that approach using data acquired on a complementary test site. RADARSAT-1 scenes acquired over an experimental watershed are used. Soil moisture and surface roughness parameters were measured in detail, coinciding with satellite overpasses. The *effective l* values calculated from the equations of Baghdadi *et al.* (2006) are used to perform forward and inverse simulations using the Integral Equation Model that are compared with radar observations and ground measurements of *SM*. The results obtained highlight the potential of the evaluated approach towards an operational radar based soil moisture estimation.

1. Introduction

Active microwave (radar) remote sensing represents an interesting alternative to classic point-based surface soil moisture (*SM*) measuring techniques. The dependence of microwave scattering over bare soil surfaces on the dielectric constant of soils allows the extraction of soil moisture information from radar observations (Ulaby *et al.*, 1982). In addition, radar observations cover large areas with a certain periodicity and have a high spatial resolution. These characteristics make radar-based soil moisture estimation very attractive to domains like hydrology, agronomy, and meteorology (Engman, 1991; Pauwels *et al.*, 2001; Schmugge *et al.*, 2002).

Radar-based *SM* estimation has been intensively studied in the last decades (for instance: Ulaby *et al.*, 1986; Altese *et al.*, 1996; Biftu and Gan, 1999; Quesney *et al.*, 2000; Moran *et al.*, 2004; Álvarez-Mozos *et al.*, 2006). Although different techniques have been developed, at present, the inversion of the Integral Equation Model (IEM) (Fung, 1994), a theoretical backscattering model with the widest range of applicability, is the most frequently followed approach for radar-based *SM* retrieval

*Corresponding author. Email: jesus.alvarez@unavarra.es

International Journal of Remote Sensing
ISSN 0143-1161 print/ISSN 1366-5901 online © 2008 Taylor & Francis
http://www.tandf.co.uk/journals
DOI: 10.1080/01431160802036367

(Altese *et al.*, 1996; Bindlish and Barros, 2000; Moran *et al.*, 2004). The IEM estimates the backscattering coefficient (σ^0) of a soil surface once its dielectric constant (ε, directly related to *SM*), roughness parameters, and sensor configuration are known. The roughness parameters required by the IEM, and most generally used in radar applications, are the standard deviation of surface heights (s), the shape of the autocorrelation function (generally assumed exponential) and the surface correlation length (l). Thus, the inversion of *SM* from σ^0 observations requires the measurement or estimation of the two roughness parameters s and l. Previous research reveals that the main problems in the estimation of *SM* through radar data seem to be related to the complicated characterisation of those roughness parameters and also to their spatial variability (Altese *et al.*, 1996; Álvarez-Mozos *et al.*, 2006).

In the case of agricultural surfaces, roughness is primarily related to tillage practices. Therefore, it should be possible to assign one set of reference roughness parameters to fields with a specific tillage condition. However, ground measurements reveal that both roughness parameters behave very differently in this sense (Álvarez-Mozos *et al.*, 2005): while s shows fairly differentiated values for different tillage classes, l remains highly variable and takes a similar range of values for all tillage classes. As a result, the uncertainties on the estimation of l are often translated into great inaccuracies in the retrieved soil moisture values (Altese *et al.*, 1996; Davidson *et al.*, 2000).

Recent studies (Baghdadi *et al.*, 2002, 2004, 2006) suggested that backscattering models needed to be calibrated to obtain *optimum* or *effective* values of parameter l that overcame the uncertainties related to its ground measurement and corrected the imperfections or limitations of the IEM. Baghdadi *et al.* (2002) obtained *effective l* values for several test fields observed under different radar configurations. Their results revealed that *effective l* values were a function of the observed s values and of radar configuration according to an exponential law. On a subsequent article, Baghdadi *et al.* (2004) extended their calibration analysis to different radar configurations in order to explore the role of the acquisition parameters (incidence angle, polarization, and frequency) and that of the surface correlation function shape. Over smooth and medium roughness conditions ($k \cdot s \leqslant 3$), the exponential function provided good results, whereas very rough surfaces were better modelled through fractal correlation functions. Results were consistent with previous calibration efforts and showed that *effective l* values were related to their corresponding s values according to exponential or power-like functions (the latter were more adequate for very rough surfaces). Besides, the coefficients of those exponential or power like functions varied depending on the acquisition parameters. On a latter study (Baghdadi *et al.*, 2006), the influence of the incidence angle on *effective l* values was further analysed on observations acquired in *C* band and *hh* and *vv* polarizations. Baghdadi *et al.* (2006) proposed the following equation to obtain *effective l* values:

$$l_{\text{eff}}(s, \theta, pp) = \alpha s^{\beta}, \tag{1}$$

where l_{eff} refers to *effective l*, θ the incidence angle, and *pp* the polarization; and α and β are coefficients that depend on θ and pp and can be calculated as:

$$\alpha_{pp} = \delta(\sin\theta)^{\mu} \tag{2}$$

$$\beta_{pp} = \eta\theta + \xi, \tag{3}$$

where δ, μ, η, and ξ are calibration coefficients. The calibration coefficients δ and ξ are dependent on the polarization, while μ and η were found to be independent: $\delta_{hh}=4.026$, $\delta_{vv}=3.289$, $\mu=-1.744$, $\eta=-0.0025$, $\xi_{hh}=1.551$ and $\xi_{vv}=1.222$ (Baghdadi *et al.*, 2006).

The results of Baghdadi *et al.* (2002, 2004, 2006) are very promising and constitute a step forward on the development of operational procedures for radar-based soil-moisture estimation. The proposed calibration improved the performance of the IEM and, furthermore, reduced the number of unknown surface parameters from three (*SM*, *s*, and *l*) to two (*SM* and *s*) facilitating their inversion from radar observations. However, the accuracy of the calibration procedure and the validity of the empirical coefficients on other agricultural areas need to be further evaluated. In this paper, a case study is presented where the approach of Baghdadi *et al.* (2006) is evaluated.

The main objective of this paper is to evaluate the validity of the presented approach using data acquired on a complementary test site. RADARSAT-1 scenes acquired over an experimental watershed are used. Soil moisture and surface roughness parameters were measured in detail, coinciding with satellite overpasses. From the equations of Baghdadi *et al.* (2006), *effective l* values are calculated, and their validity is evaluated using IEM simulations.

2. Materials and methods

2.1 *Test site*

The research was carried out over a small agricultural watershed located in the region of Navarre (North of Spain) called *La Tejería* (figure 1). This watershed is a part of the Experimental Agricultural Watershed Network of the local Government

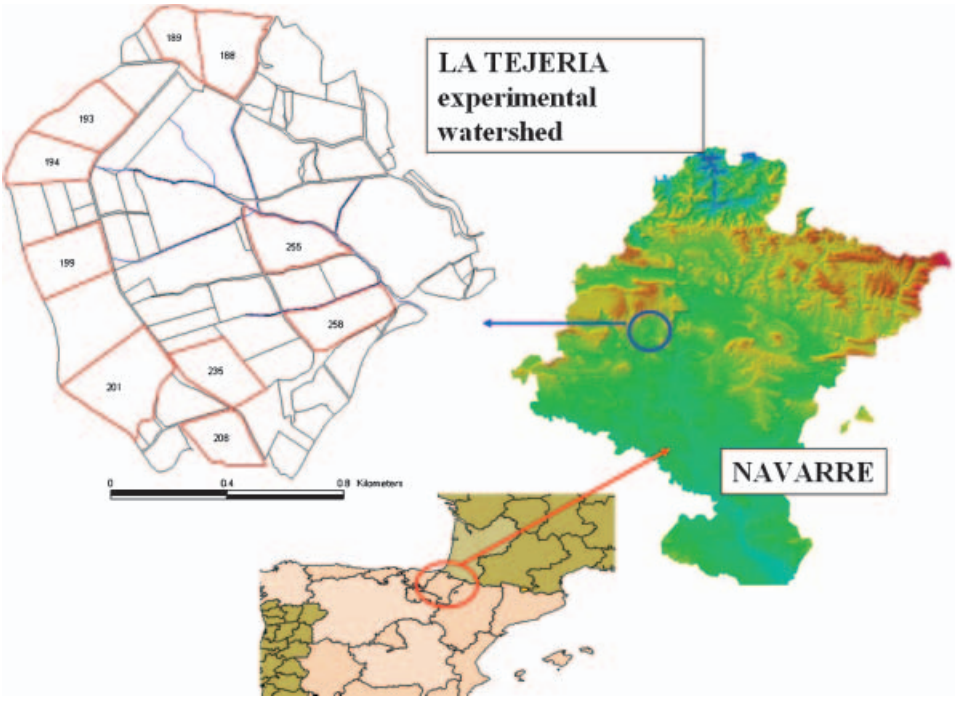

Figure 1. Location of *La Tejería* experimental watershed. The control fields are highlighted.

of Navarre, established in 1993. The geographical coordinates of the watershed outlet are 42°44′10.6″ N and 1°56′57.2″ W. The watershed covers approximately 170 ha with homogeneous slopes of about 12%, and an altitude ranging from 496 to 649 m. Its climate is humid sub-Mediterranean, with a mean annual temperature of 13°C. The average annual rainfall is about 700 mm distributed over approximately 105 days.

The soils have clayey textures (43% clay, 5% sand, 52% silt) and depths around 1 m. The watershed is almost completely cultivated, and the hedgerows and streams are the only areas covered by natural vegetation. Winter cereal crops are the main cropping system. Generally, tillage and soil preparation practices start in September, crops are sown at the beginning of November, and harvest takes place around the end of June.

The watershed had been equipped with an automated meteorological and hydrological station. The station has provided precipitation and flow discharge data on a 10-min basis and daily water quality data since 1994.

2.2 *Radar scenes*

Five RADARSAT-1 SGF scenes (*C* band, HH polarization) were used in this study. The scenes were acquired over Navarre during spring 2003 (27 February, 6 March, 23 March, 30 March, and 2 April). Beam modes S1 and S2 were selected for their lower incidence angles (on average 23.5° and 27.5°, respectively). Radar observations acquired at low incidence angles and direct polarization are more appropriate for soil moisture retrieval, since vegetation-induced attenuation, as well as surface roughness influence, is minimized (Ulaby *et al.* 1982).

2.3 *Ground measurements*

Coinciding with image acquisitions, surface soil moisture and roughness measurements were performed over the catchment. The moisture content of the top 10 cm of the soil was measured on each image acquisition day using a calibrated TDR probe. Sixteen control fields were selected over the catchment, and their size ranged from 1.3 to 7.3 ha, with an average value of 4.2 ha. A minimum of three sampling points were monitored on each control field (on each point, three TDR measurements were performed), making a total of 60 sampling points along the catchment on each scene acquisition day. The *SM* values observed reflected rainfall patterns throughout the experimental campaign.

Surface roughness was measured using a 1-m-long needle profilometer with a sampling interval of 2 cm. Surface profiles were collected parallel to the tillage row direction, only if a clear row pattern was evidenced. Over those fields that did not present a clear oriented roughness pattern, profiles were collected in all directions. The aim was to reflect only the random component of roughness, which is the one directly involved in the backscattering process (Ulaby *et al.*, 1986). Surface roughness was considered to be invariable in time because the time between acquisitions is small. Besides, roughness was also assumed to be homogeneous over fields belonging to each tillage or crop class. Four tillage classes were identified: (a) 'Rolled vegetables': very smooth soils compacted with a compacting roller, chickpeas and beans starting to germinate at the end of the period, (b) 'Rolled cereal': wheat and barley fields where a compacting roller was applied after sowing, (c) 'Cereal': conventionally sown wheat and barley fields, and (d) 'Mouldboard': very rough fields ploughed with a mouldboard. Measured parameters are shown in table 1.

Table 1. Ground measured moisture and roughness parameters.

Tillage class	*SM* range ($cm^3\,cm^{-3}$)	No. of fields	No. of profiles	Roughness parameters					
				s range (cm)	Average *s* (cm)	σ_s (cm)	*l* range (cm)	Average *l* (cm)	σ_l (cm)
Rolled vegetables	0.13–0.38	2	16	0.26–0.68	0.47	0.09	1.40–12.12	2.44	2.84
Rolled cereal	0.16–0.36	2	20	0.53–1.37	0.89	0.27	1.06–13.03	3.62	3.26
Cereal	0.13–0.39	11	48	0.51–2.01	1.05	0.34	1.21–10.98	3.49	2.63
Mouldboard	0.17–0.27	1	4	1.95–3.46	2.57	0.72	5.40–10.81	7.41	2.35

For each tillage class, the soil moisture (*SM*) range (min–max), number of control fields, and measured profiles are given along with the range (min–max), average, and standard deviation (σ) of the *s* and *l* parameters.

During this period, the fields that belonged to 'Cereal' and 'Rolled cereal' crop classes presented an emerging cereal crop (the rest had no vegetation). The characteristics of this vegetation cover were estimated using some reference ground measurements and a Landsat-7 ETM+ scene acquired on 17 March 2003. On average, the LAI of the cereal cover ranged between 2.15 at the beginning of the research period and 3.71 at the end, and the vegetation water content M_V ranged between $0.66\,kg\,m^{-2}$ and $1.32\,kg\,m^{-2}$. Further details on the experimental period can be obtained in Álvarez-Mozos *et al.* (2006).

2.4 *Image processing*

Radar scenes were processed following standard procedures. The five RADARSAT-1 SGF scenes were calibrated to obtain backscattering coefficient (σ^0) values following the standard approach of Shepherd (2000). The local incidence angle was calculated taking into account the topography (Ulander, 1996). Next, scenes were speckle-filtered and geocoded following the ground control point approach. Finally, field average σ^0 values were calculated from each scene. Average σ^0 values were calculated in linear units and next transformed to dB. As explained most of the fields in the catchment showed an early cereal crop canopy. The attenuation that such a canopy might produce on the observed σ^0 values was corrected by means of a semi-empirical Water Cloud model (Attema and Ulaby, 1978; Álvarez-Mozos *et al.*, 2006). Thus, the σ^0 values analysed in the rest of the study correspond to the soil contribution to the backscatter.

2.5 *Calculation of effective l values*

Following the approach proposed Baghdadi *et al.* (2006) *effective l* (l_{eff}) values were calculated (using equations (1)–(3)) for the different control fields, using as input the local incidence angle, polarization, and ground measured *s* values. Obtained l_{eff} values were later compared with their corresponding ground measured *l* values.

2.6 *Inversion of calibrated l values*

To compare and evaluate the l_{eff} values calculated with equation (1), calibrated *l* (l_{cal}) values were obtained using the IEM. Following a similar approach to that of Baghdadi *et al.* (2002, 2004, 2006) l_{cal} values were retrieved from σ^0 observations using the IEM and *s* and *SM* measurements. The IEM inversion was performed through a Newton–Raphson iterative algorithm. Depending on the sensor configuration and surface conditions, two solutions can be obtained (l_{cal1} and l_{cal2}) that ensure good agreement between the IEM and the σ^0 observations (figure 2). Baghdadi *et al.* (2006) recommended using the higher value (l_{cal2}), since it provides a better physical behaviour of σ^0 as a function of *s*. Inverted l_{cal2} values were later compared with the calculated l_{eff} values.

3. Results

The l_{eff} values obtained for each tillage class are summarized in table 2. The calculated l_{eff} takes different values depending on its corresponding *s*, local incidence angle of each field, and polarization of the scene. The class average l_{eff} values and their variability increase as the tillage class gets rougher. It must be noted that only class average *s* values were measured, so the differences observed in the calculated

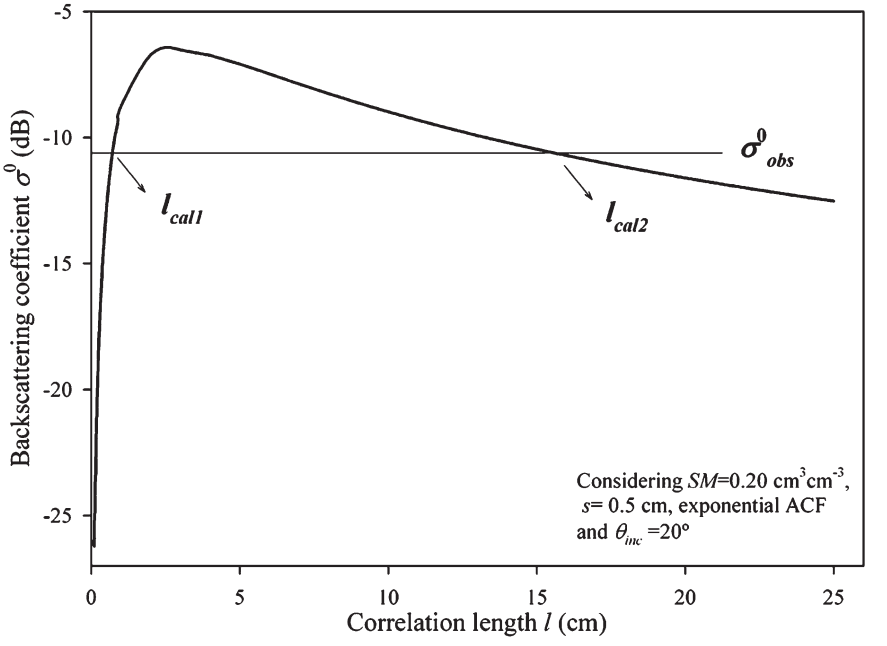

Figure 2. Sensitivity of the backscattering coefficient σ^0 to the correlation length l. Obtained from IEM simulations.

Table 2. Calculated class average effective l (l_{eff}) values.

Tillage class	θ_{inc} range (°)	l_{eff} range (cm)	Average l_{eff} (cm)	σ_{leff} (cm)
Rolled vegetables	14.37–27.92	5.02–14.87	8.66	3.61
Rolled cereal	16.25–27.63	12.97–31.27	21.30	6.13
Cereal	13.92–28.67	15.55–52.07	28.17	9.67
Mouldboard	13.81–28.59	58.97–206.25	142.75	63.08

The local incidence angle (θ_{inc}) range is given along with the l_{eff} range, its average value, and standard deviation (σ_{leff}).

l_{eff} values are a consequence of the differences in the local incidence angle of each field. Large incidence angles give larger l_{eff} values. Besides, the influence of the incidence angle on l_{eff} is more prominent over surfaces with large s values. As expected, no clear relation was evidenced between ground measurements of parameter l and their corresponding l_{eff} values (figure 3).

To evaluate the validity of the method, the IEM was applied using l_{eff} to estimate backscattering values that could be compared with radar observations (figure 4). The estimated σ^0 values agreed with RADARSAT-1 observations (figure 4). In the 'Cereal' tillage class, the agreement was close, although an overestimation of approximately 2 dB could be evidenced at low backscatter values. The agreement was also adequate in the class 'Rolled cereal'. Some fields that belonged to the class 'Rolled vegetables' showed lower σ^0 estimations than observed on the RADARSAT-1 scene, but the agreement was in general satisfactory. The 'Mouldboard' field showed the weakest agreement. Even if the correlation between estimated and observed σ^0 values was positive, there was an offset in the estimations of around 3–4 dB.

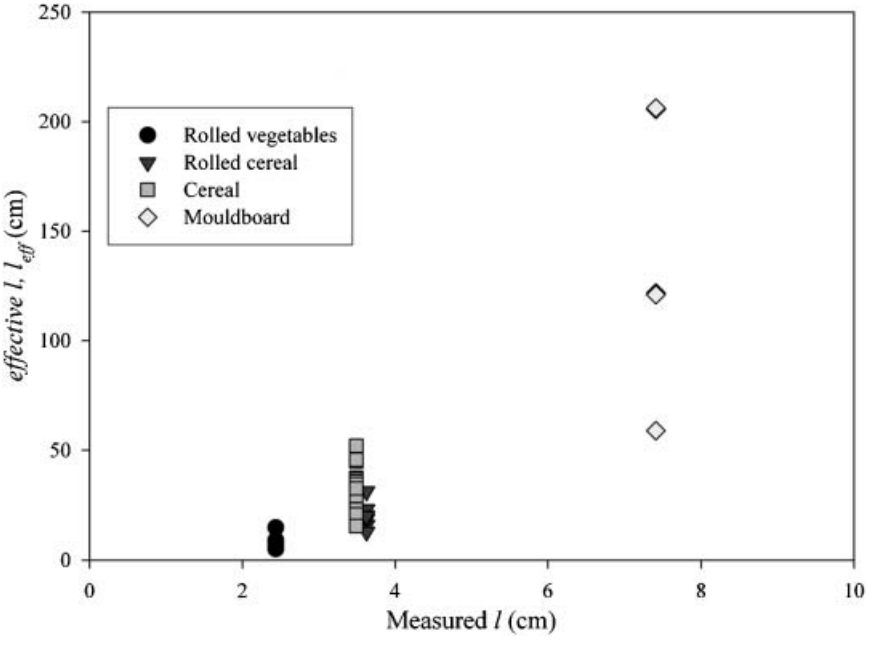

Figure 3. Comparison between calculated effective correlation length values l_{eff} and ground measured l for each control field.

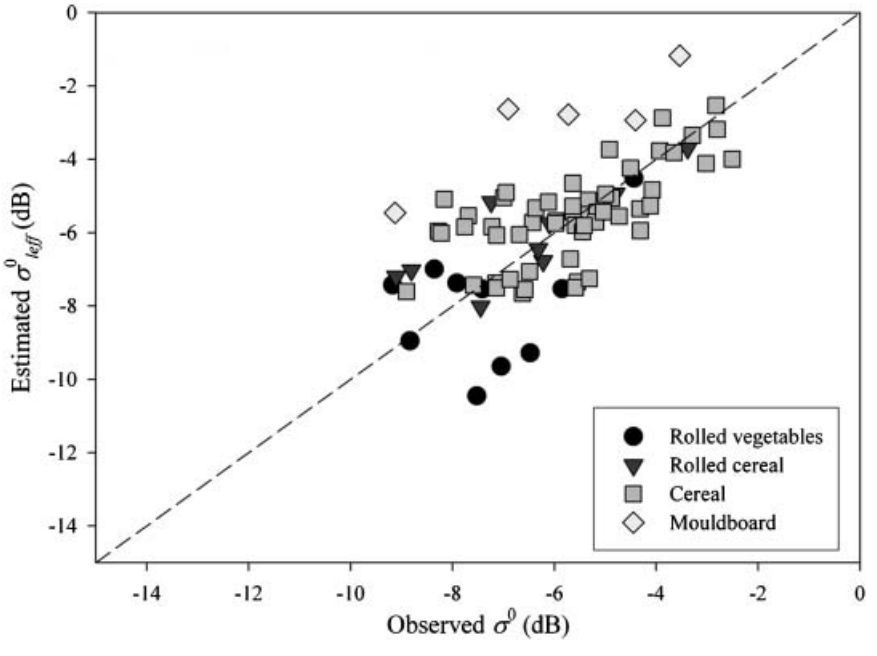

Figure 4. Estimated backscattering coefficient using the IEM and l_{eff} values ($\sigma^0{}_{\text{leff}}$) versus radar observations.

The IEM was next applied using ground measured l values to compare with the IEM results obtained using l_{eff}. The estimations obtained were also plotted against SAR observations (figure 5). The root mean square errors (RMSE) of the

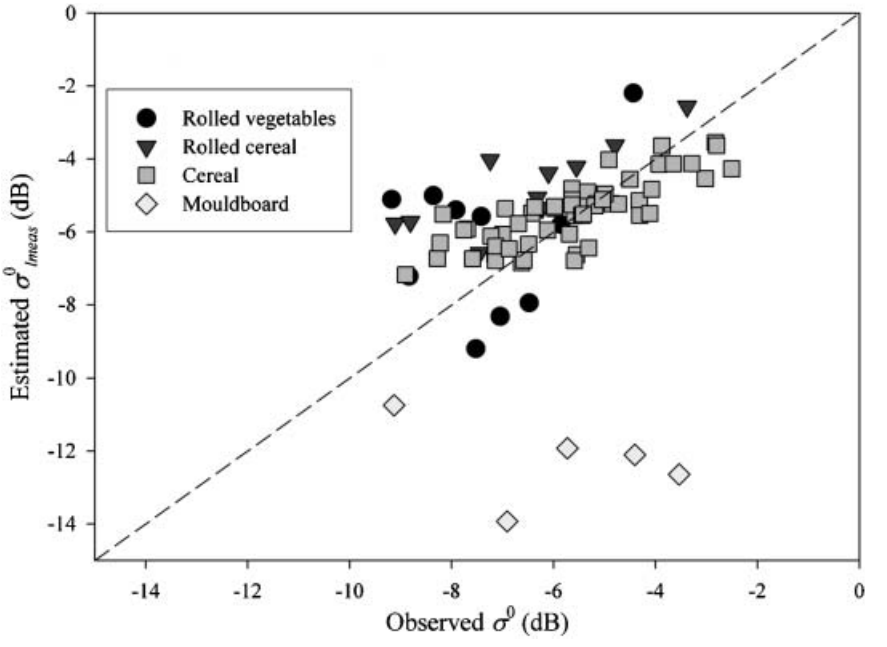

Figure 5. Estimated backscattering coefficient using the IEM and ground measured l values (σ^0_{lmeas}) versus radar observations.

estimations were then computed for each tillage class on both cases (IEM simulations using l_{eff} values and using measured l values) (table 3). The agreement between observations and estimated σ^0 values using l ground measurements was very similar to that obtained using l_{eff} values (figure 5). The main difference was observed in the class 'Mouldboard' where the backscattering coefficient was severely underestimated when ground measured l values were used.

The RMSE values calculated summarize the results (table 3). In general, RMSE values were similar using l ground measurements or l_{eff} values. The differences observed were small except for the 'Mouldboard' class.

The calculated l_{eff} values were plotted against the l_{cal2} values retrieved inverting the IEM (figure 6). The comparison showed a good agreement for low l_{eff} values, but at larger values l_{eff} was lower than the retrieved l_{cal2}. The underestimation could be a consequence of the reduced sensitivity of σ^0 to l at large l values. This reduced sensitivity can cause a poorer performance of the approach over rough surfaces, but further studies are needed to thoroughly analyse the approach on rough conditions.

Table 3. Root mean square error RMSE values obtained between σ^0 observations and estimations using l_{eff} and l_{meas} in IEM simulations.

	σ^0 RMSE (dB), using l_{eff}	σ^0 RMSE (dB), using l_{meas}
Period 1		
Rolled vegetables	1.15	0.97
Rolled cereal	1.10	2.02
Cereal	1.77	2.27
Mouldboard	2.20	6.82

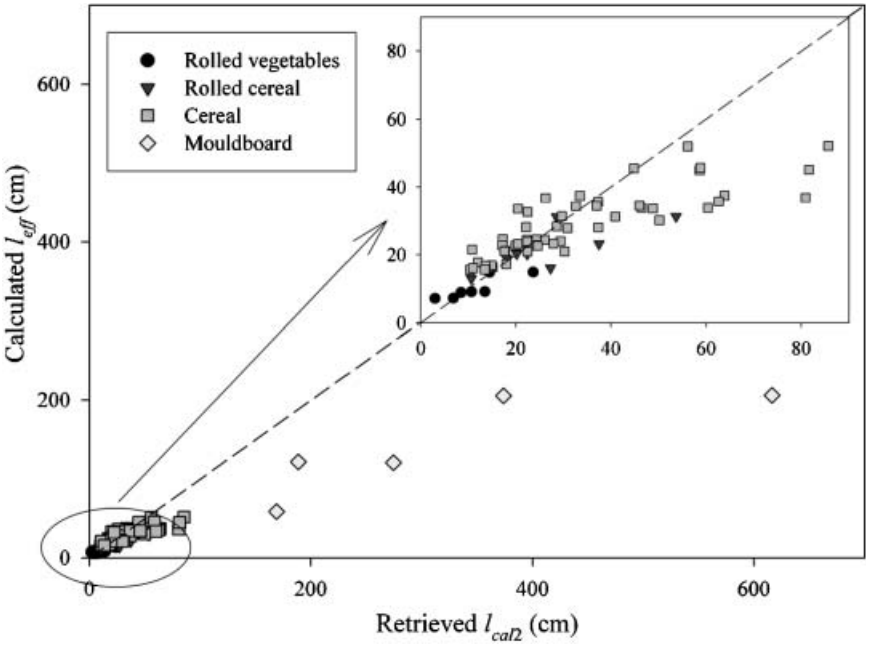

Figure 6. Calculated l_{eff} compared to retrieved l_{cal2} for each control field. Retrieved l_{cal2} values were obtained inverting the IEM using RADARSAT-1 σ^0 observations and *SM* and *s* ground measurements. Symbols represent the different tillage classes.

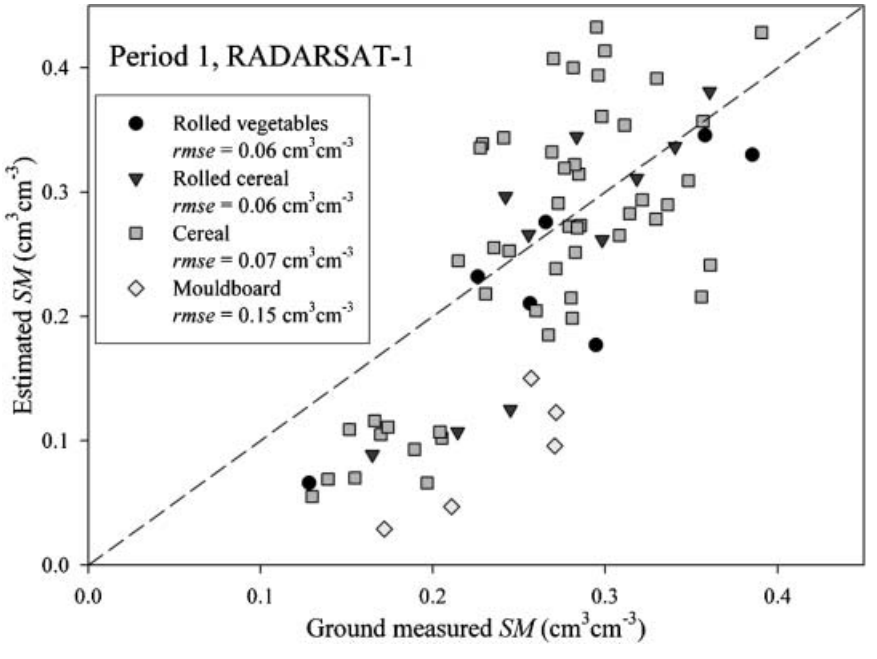

Figure 7. Estimated versus ground measured soil moisture (*SM*). The *SM* is estimated inverting the IEM using RADARSAT-1 observations, *s* measurements and l_{eff} values. Symbols represent the different tillage classes. The root mean square error (*rmse*) of the estimations is given for each class.

Finally, the l_{eff} values were used to invert the soil moisture content of the control fields using the IEM and the σ^0 observations. Obtained results were plotted in figure 7. Under dry conditions, *SM* was underestimated, but in general the results are promising. The class average RMSE of the estimated *SM* ranged between $0.06\,cm^3\,cm^{-3}$ and $0.15\,cm^3\,cm^{-3}$. These results are satisfactory, especially taking into account that *SM* was estimated at the field scale and that the control fields had an average size of around 4 ha. It must be pointed out that *s* values were measured considering homogeneous roughness conditions for each tillage class. Thus, a class average *s* estimation was the only necessary roughness parameter to invert *SM* from radar observations using this approach.

4. Conclusions

The results of this study show that the methodology proposed by Baghdadi *et al.* (2006) for the calculation of the effective correlation length l_{eff} is very promising. The simulations performed with the IEM using l_{eff} values agreed reasonably with observations, on both the forward (estimation of σ^0) and the inverse (retrieval of *SM*) mode. On the latter, the errors in the estimation of *SM* ranged between $0.06\,cm^3\,cm^{-3}$ and $0.15\,cm^3\,cm^{-3}$. It would be convenient to perform additional evaluations of the approach with alternative observations and data sets, especially over rough conditions, to thoroughly evaluate its validity.

Acknowledgments
The authors would like to thank the reviewers for their valuable comments. This study was partly funded by the Spanish Government's National Scientific Research, Development and Technological Innovation Plan, project code REN2003-03028/HID; the Canadian Space Agency's Data for Research Use program project No. DRU-10-02.

References

Altese, E., Bolognani, O., Mancini, M. and Troch, P.A., 1996, Retrieving soil moisture over bare soil from ERS 1 synthetic aperture radar data: Sensitivity analysis based on a theoretical surface scattering model and field data. *Water Resources Research*, **32**, pp. 653–661.

Álvarez-Mozos, J., Casali, J., Gonzalez-Audicana, M. and Verhoest, N.E.C., 2006, Assessment of the operational applicability of RADARSAT-1 data for surface soil moisture estimation. *IEEE Transactions on Geoscience and Remote Sensing*, **44**, pp. 913–924.

Álvarez-Mozos, J., Larrañaga, A. and Casali, J., 2005, Measurement and analysis of soil surface roughness over agricultural areas using a laser profile meter. Analysis of the temporal evolution of roughness as influenced by rainfall. In *Sixth International Conference on Geomorphology, Geomorphology in Regions of Environmental Contrasts, Zaragoza (Spain)*, Abstracts Volume, p. 177.

Attema, E.W.P. and Ulaby, F.T., 1978, Vegetation modelled as a water cloud. *Radio Science*, **13**, pp. 357–364.

Baghdadi, N., Gherboudj, I., Zribi, M., Sahebi, M., King, C. and Bonn, F., 2004, Semi-empirical calibration of the IEM backscattering model using radar images and moisture and roughness field measurements. *International Journal of Remote Sensing*, **25**, pp. 3593–3623.

Baghdadi, N., King, C., Chanzy, A. and Wigneron, J.P., 2002, An empirical calibration of the Integral Equation Model based on SAR data, soil moisture and surface roughness

measurement over bare soils. *International Journal of Remote Sensing*, **23**, pp. 4325–4340.

BAGHDADI, N., HOLAH, N. and ZRIBI, M., 2006, Calibration of the Integral Equation Model for SAR data in C-band and HH and VV polarizations. *International Journal of Remote Sensing*, **27**, pp. 805–816.

BIFTU, G.F. and GAN, T.Y., 1999, Retrieving near-surface soil moisture from RADARSAT SAR data. *Water Resources Research*, **35**, pp. 1569–1579.

BINDLISH, R. and BARROS, A.P., 2000, Multifrequency soil moisture inversion from SAR measurements with the use of IEM. *Remote Sensing of Environment*, **71**, pp. 67–88.

DAVIDSON, M.W.J., LE TOAN, T., MATTIA, F., SATALINO, G., MANNINEN, T. and BORGEAUD, M., 2000, On the characterization of agricultural soil roughness for radar remote sensing studies. *IEEE Transactions on Geoscience and Remote Sensing*, **38**, pp. 630–640.

ENGMAN, E.T., 1991, Applications of Microwave remote sensing of soil moisture for water resources and agriculture. *Remote Sensing of Environment*, **35**, pp. 213–226.

FUNG, A.K., 1994, *Microwave Scattering and Emission Models and Their Applications* (Norwood, MA: Artech House).

MORAN, M.S., PETERS-LIDARD, C.D., WATTS, J.M. and MCELROY, S., 2004, Estimating soil moisture at the watershed scale with satellite-based radar and land surface models. *Canadian Journal of Remote Sensing*, **30**, pp. 805–826.

PAUWELS, V.R.N., HOEBEN, R., VERHOEST, N.E.C. and DE TROCH, F.P., 2001, The importance of the spatial patterns of remotely sensed soil moisture in the improvement of discharge predictions for small scale basins through data assimilation. *Journal of Hydrology*, **251**, pp. 88–102.

QUESNEY, A., Le HÉGARAT-MASCLE, S., TACONET, O., VIDAL-MADJAR, D., WIGNERON, J.P., LOUMAGNE, C. and NORMAND, M., 2000, Estimation of watershed soil moisture index from ERS/SAR data. *Remote Sensing of the Environment*, **72**, pp. 290–303.

SCHMUGGE, T.J., KUSTAS, W.P., RITCHIE, J.C., JACKSON, T.J. and RANGO, A., 2002, Remote sensing in hydrology. *Advances in Water Resources*, **25**, pp. 1367–1385.

SHEPHERD, N., 2000, *Extraction of Beta Nought and Sigma Nought From RADARSAT CDPF Products. Technical Report* (Ottawa: Altrix Systems).

ULABY, F.T., MOORE, R.K. and FUNG, A.K., 1982, *Microwave Remote Sensing, Active and Passive, Volume I: Radar Remote Sensing Fundamentals and Radiometry* (Norwood, MA: Artech House).

ULABY, F.T., MOORE, R.K. and FUNG, A.K., 1986, *Microwave Remote Sensing, Active and Passive, Volume III: from Theory to Applications* (Norwood, MA: Artech House).

ULANDER, L., 1996, Radiometric slope correction of synthetic aperture radar images. *IEEE Transactions on Geoscience and Remote Sensing*, **34**, pp. 1115–1122.